Manufacturer's Association (CMA) with A. F. Tuck, Project Scientist. An in-depth analysis of the results from AAOE mission, as well as the NOZE II series, appears in a special issue of *J. Geophys. Res.* **94**, 11,181 (1989).
17. A series of papers trace this development: J. G. Anderson, J. J. Margitan, D. H. Stedman, *Science* **198**, 501 (1977); J. G. Anderson, H. J. Grassl, R. E. Shetter, J. J. Margitan, *J. Geophys. Res.* **85**, 2869 (1980); J. J. Schwab and J. G. Anderson, *J. Quant. Spectrosc. Rad. Transfer* **27**, 445 (1982); W. H. Brune and J. G. Anderson, *Geophys. Res. Lett.* **13**, 1391 (1986); W. H. Brune, E. M. Weinstock, J. G. Anderson, *ibid.* **15**, 144 (1988).
18. See the discussion in W. H. Brune, J. G. Anderson, K. R. Chan, *J. Geophys. Res.* **94**, 16,639 (1989); *ibid.*, p. 16,649; D. W. Toohey, J. G. Anderson, W. H. Brune, K. R. Chan, *Geophys. Res. Lett.* **17**, 513 (1990).
19. M. H. Proffitt *et al.*, *J. Geophys. Res.* **94**, 16,547 (1989).
20. Potential temperature is defined by and computed from the expression $\theta = T(P_S/P)^x$, where T is the observed temperature of the air parcel, P_S is the surface pressure, P is the actual pressure of the air parcel, and x is the ratio of the gas constant, R, to the specific heat at constant pressure, C_p. A heuristic definition of potential temperature is that it is the temperature of an air parcel brought adiabatically from the point of interest to sea level.
21. For a complete discussion of the dynamics of polar vortices and a discussion of dynamical exchange, see M. R. Schoeberl and D. L. Hartmann, *Science* **251**, 46 (1991).
22. D. W. Fahey *et al.*, *J. Geophys. Res.* **94**, 16,665 (1989).
23. J. R. Podolske, M. Loewenstein, S. E. Strahan, K. R. Chan, *ibid.*, p. 16,767; L. E. Heidt, J. F. Vedder, W. H. Pollock, R. A. Lueb, B. E. Henry, *ibid.*, p. 11,599.
24. K. K. Kelly *et al.*, *ibid.*, p. 11,317.
25. J. G. Anderson, W. H. Brune, M. H. Proffitt, *ibid.*, p. 11,465.
26. O. B. Toon, P. Hamill, R. P. Turco, J. Pinto, *Geophys. Res. Lett.* **13**, 1284 (1986); P. J. Crutzen and F. Arnold, *Nature* **324**, 651 (1986); M. B. McElroy, R. J. Salawitch, S. C. Wofsy, *Geophys. Res. Lett.* **13**, 1296 (1986); L. R. Poole and M. P. McCormick, *J. Geophys. Res.* **93**, 8423 (1988).
27. M. J. Molina, T. Tso, L. T. Molina, F. C. Y. Wang, *Science* **238**, 1253 (1987); M. A. Tolbert, M. J. Rossi, R. Malhotra, D. M. Golden, *ibid.*, p. 1258.
28. M. R. Schoeberl *et al.*, *J. Geophys. Res.* **94**, 16,815 (1989).
29. J. G. Anderson *et al.*, *ibid.*, p. 11,480.
30. The opposing views on whether the antarctic vortex more nearly approximates (i) an isolated air mass or (ii) a flow reactor are represented, respectively, by (i) D. L. Hartmann *et al.*, *J. Geophys. Res.* **94**, 16,779 (1989); M. R. Schoeberl *et al.* (*28*); and (ii) A. F. Tuck *et al.*, *ibid.*, p. 11,687; M. J. Proffitt *et al.*, *ibid.*, p. 16,797; E. F. Danielsen, *J. Atmos. Sci.*, **47**, 2013 (1990).
31. M. H. Proffitt, D. W. Fahey, K. K. Kelly, A. F. Tuck, *Nature* **342**, 233 (1989).
32. D. E. Anderson and S. A. Lloyd, *J. Geophys. Res.* **95**, 7429 (1990); D. E. Anderson, *Planet. Space Sci.* **31**, 1517 (1983).
33. S. P. Sander, R. R. Friedl, Y. L. Yung, *Science* **245**, 1095 (1989); M. Trolier, R. L. Mauldin III, A. R. Ravishankara, *J. Phys. Chem.* **94**, 4896 (1990).
34. M. Birk *et al.*, *J. Chem. Phys.* **91**, 6588 (1989).
35. M. J. Molina, A. J. Colussi, L. T. Molina, R. N. Schindler, T.-L. Tso, *Chem. Phys. Lett.* **173**, 310 (1990).
36. R. Watson was primarily responsible for organizing and expediting the Airborne Antarctic Ozone Experiment (AAOE). A. Tuck orchestrated the ER-2 and DC-8 operations, the aircraft trajectory, the British Meteorology Office weather forecasts, and the science meetings in Punta Arenas, Chile, during the mission. Field support for this mission came both from the NOAA Aeronomy Lab staff, notably T. Thompson and R. Winkler, and from the NASA Ames staff led by E. Condon and G. Ferry. We also thank N. Hazen and J. Demusz for the optical-mechanical and electronic design of the instrument, and N. Allen and M. Mueller, who developed the software for both the flight system and data reduction. P. Soderman played a critical role in the conception of the double-ducted arrangement used in the experiment. A. Schmeltekopf gave us invaluable advice. B. Ferguson helped with the ER-2 aircraft. We also thank J. Arveson and J. Barrilleaux. Finally, we thank the pilots: R. Williams, J. Hoyt, J. Barrilleaux, and D. Krumrey. Research was supported by NASA contract NASW 3960 and NAG2-443.

The Dynamics of the Stratospheric Polar Vortex and Its Relation to Springtime Ozone Depletions

MARK R. SCHOEBERL AND DENNIS L. HARTMANN

Dramatic springtime depletions of ozone in polar regions require that polar stratospheric air has a high degree of dynamical isolation and extremely cold temperatures necessary for the formation of polar stratospheric clouds. Both of these conditions are produced within the stratospheric winter polar vortex. Recent aircraft missions have provided new information about the structure of polar vortices during winter and their relation to polar ozone depletions. The aircraft data show that gradients of potential vorticity and the concentration of conservative trace species are large at the transition from mid-latitude to polar air. The presence of such sharp gradients at the boundary of polar air implies that the inward mixing of heat and constituents is strongly inhibited and that the perturbed polar stratospheric chemistry associated with the ozone hole is isolated from the rest of the stratosphere until the vortex breaks up in late spring. The overall size of the polar vortex thus limits the maximum areal coverage of the annual polar ozone depletions. Because it appears that this limit has not been reached for the Antarctic depletions, the possibility of future increases in the size of the Antarctic ozone hole is left open. In the Northern Hemisphere, the smaller vortex and the more restricted region of cold temperatures suggest that this region has a smaller theoretical maximum for column ozone depletion, about 40 percent of the currently observed change in the Antarctic ozone column in spring.

THE STRATOSPHERE IS THE ATMOSPHERIC REGION JUST above the tropopause, between roughly 12 and 50 km (100 and 1 mb in pressure). Within this region the air temperature generally increases with altitude rising from −50°C or lower at the tropopause to greater than −20°C at 50 km. The relative warmth of the stratosphere results from the absorption of solar ultraviolet radiation by O_3, which has its highest mixing ratio in the stratosphere. This heating by solar absorption is balanced by cooling through emission of thermal infrared radiation, primarily from the 15-μm band of CO_2. After the autumnal equinox, the polar regions fall into darkness and the solar ultraviolet heating ceases. Emission of thermal radiation quickly cools the polar stratosphere to temper-

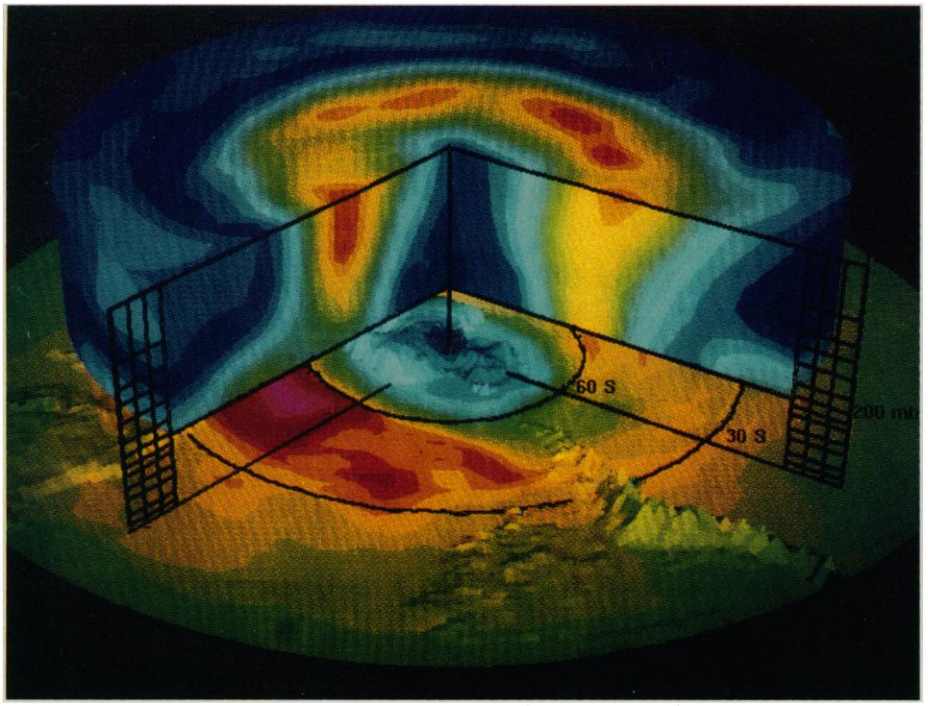

Fig. 1. The Antarctic polar vortex and the ozone hole on 7 October 1989. Upper part of the figure (cylindrical structure with missing wedge) shows the wind speeds. Wind speeds range from 0 (dark blue) to 80 m s^{-1} (red); the cylinder is centered on the south pole. Surface plot below shows the orography not to scale; the Andes are the chain of mountains moving from the center of the figure to the lower right, Antarctica is at the center, and southern Africa is on the left. The surface color scheme shows total ozone, and blue colors indicate values below 200 Dobson Units (DU). Grids indicate standard pressure levels; the wind speed plot starts at 200 mb (10 km) and extends to 10 mb (30 km). Latitudes are shown at 30° and 60°. The figure shows the containment of the ozone hole by the strong wind belt or polar vortex.

atures much lower than those of the mid-latitude stratosphere. A latitudinal pressure gradient then develops between the pole and mid-latitudes, which combined with Earth's rotation, produces a circumpolar belt of westerly winds referred to as the polar night jet or polar vortex. Wind speeds in this jet may exceed 100 m s^{-1}. In this article, we discuss the recent evidence on the dynamics of the polar vortex and its relationship to polar ozone depletions.

Although temperatures within the polar vortex in wintertime are basically driven by radiative processes, they are also determined by dynamics and the transport of heat by atmospheric motions. Zonally symmetric circulations are relatively inefficient at transporting heat in a rotating fluid such as Earth's atmosphere (*1*). Thus in order for temperatures within the polar vortex to depart substantially from radiatively determined values, thermal transport by wave motions is required. The most important waves for mixing in the stratosphere are planetary-scale Rossby waves, or planetary waves, which propagate upward from the troposphere. Stratospheric planetary waves, first described in the early 1960s (*2*), are associated with large amplitude quasi-stationary stratospheric features such as the Aleutian anticyclone. Planetary waves are also responsible for the intermittent breakdowns of the polar-vortex structure called sudden stratospheric warmings. In the Northern Hemisphere, midwinter sudden stratospheric warmings often lead to a temporary reversal of the north-south zonal mean temperature gradient (*3*).

Chemistry in the Polar Vortex

Under normal winter conditions in the lower stratosphere, the temperatures within the polar vortex fall low enough that clouds of nitric acid trihydrate and ice can form despite the dryness of the stratosphere (2 to 4 ppm mixing ratio of H_2O). These clouds are referred to generically as polar stratospheric clouds (PSCs) (*4*). Pure ice clouds form near −88°C at 50-mb pressure (roughly 20 km), an extreme temperature that is rarely maintained for long periods except in the Antarctic winter stratosphere. The clouds of nitric acid trihydrate form at temperatures roughly 10°C warmer (*5*) and thus probably account for most of the PSCs.

The PSCs are now recognized as the key ingredient in the springtime destruction of ozone and the formation of the ozone hole (*6*). They are the sites for a group of heterogeneous reactions that perturb the normal gas-phase chemistry in the polar region. The most important heterogeneous reaction is that which converts the relatively unreactive chlorine species, chlorine nitrate and hydrochloric acid (the dominant chlorine reservoirs), to molecular chlorine and nitric acid,

$$ClONO_2 + HCl \xrightarrow{M} HNO_3 + Cl_2 \quad (1)$$

where M is a third body molecule or particle. The molecular chlorine is photolyzed in the spring sunlight, and atomic chlorine quickly reacts with O_3 to from the chlorine monoxide radical (ClO). Substantial catalytic O_3 destruction at rates of 0.5 to 1% per day begins with the formation of the dimer $(ClO)_2$ and the reaction of ClO with bromine monoxide (BrO) (*7*, *8*) (also see accompanying article by Anderson *et al.*).

Widespread ozone destruction during the Antarctic spring requires that the air first be chilled below −78°C for a sufficient time that the polar stratospheric clouds can effect the conversion of chlorine from the inactive reservoir species to the radical species that attack ozone. Elevated concentrations of ClO and Cl must then be maintained long enough to reduce substantially the O_3 concentration (*8*). Such conditions occur over widespread regions of the Antarctic lower stratosphere, but not as extensively in the Arctic. Nonetheless, high levels of ClO have been detected in the Arctic stratosphere along with evidence of O_3 loss (*9*).

To prevent the conversion of ClO back to unreactive chlorine nitrate through the reaction of ClO with NO_2, active nitrogen compounds must be suppressed. The formation of PSCs sequesters HNO_3 in trihydrate particles after the heterogeneous reaction by condensation and also denitrifies the vortex air. The observed ozone destruction in both hemispheres is therefore contingent on the stratosphere remaining denitrified during the period of ozone loss, and this means that mid-latitude air containing reactive nitrogen

M. R. Schoeberl is at the National Aeronautics and Space Administration, Goddard Space Flight Center, Greenbelt, MD 20771. D. L. Hartmann is in the Department of Atmospheric Sciences, University of Washington, Seattle, WA 98195.

compounds cannot be mixed into the polar vortex. The dynamical characteristics of the polar vortex provide this chemical isolation, and the ozone hole develops poleward of the latitude of strongest westerly winds (Fig. 1).

Structure and Evolution of the Polar Vortex

The stratospheric polar vortex develops poleward and above the subtropical jet (Fig. 2B). The structure of the polar vortex is different in the two hemispheres. The winter jet in the Southern Hemisphere is far stronger than its northern counterpart and is associated with a larger poleward temperature decrease in the lower stratosphere. Polar cold pools in the lower stratosphere are evident in both hemispheres (Fig. 2A) and are located where PSCs are usually observed (*4*). The comparatively larger cold temperature region in the Antarctic stratosphere implies that PSCs form more effectively there than in the Northern Hemisphere and that there is a larger region for heterogeneous reactions to occur.

The seasonal evolution of polar temperatures as cold as −70°C closely follows the onset of polar night (Fig. 3). The Southern Hemisphere thermal response is mainly radiative, in that it follows the seasonal changes of insolation fairly closely. The Northern Hemisphere begins to show a departure from this path in mid-December. These interhemispheric differences in stratospheric climatology can be traced to the more frequent disruption of the boreal vortex by planetary waves.

Planetary waves are forced in the troposphere by large-scale orographic and thermal contrasts and can propagate into the stratosphere only when westerly winds are present (*2*). In the Northern Hemisphere, the great mountain masses of Asia and North America send large-amplitude Rossby waves upward to stir the stratosphere. The continent of Antarctica, however, is almost centered on the South Pole and is surrounded by ocean. Only the rather narrow band of the Andes disturbs the east-west symmetry of the surface conditions, and these mountains have little effect on the symmetry of the Austral polar vortex.

After the autumnal equinox, radiative processes cool the polar stratosphere and a symmetric overturning begins with strong downward motion in the polar regions and weak rising motion elsewhere. Downward motion in the polar region warms the air through adiabatic compression, partially offsetting the radiative cooling which would otherwise take the temperature to −90°C or below (*11*). The descending air within the vortex carries with it the trace chemical composition of the upper stratosphere. Below 30 km the vortex temperature approaches radiative equilibrium, and the rate of descent within the vortex decreases. Outside the cold vortex, however, air is being laterally mixed by planetary waves. Thus, even though the diabatic descent may be more rapid exterior to the vortex (because the air outside the vortex is warmer and radiatively cooling rates are larger), this descent is largely countered by rapid lateral mixing by planetary waves. Thus during winter an apparent differential vertical displacement of air between the vortex exterior and interior progressively develops. Aircraft measurements show that air inside the vortex appears to be displaced downward by 2 to 3 km compared to air exterior to the vortex on the same pressure surface (*12*). As we will describe below, these gradients are not produced by mean vertical motions alone, but by the combined effects of mean vertical motion and lateral mixing by planetary waves.

The amplitude of upward-propagating planetary waves is observed to increase with altitude as does the magnitude of their heat transport. This increase in heat flux is seen in the weakening of the pole to mid-latitude temperature gradient above 25 to 30 km (Fig. 2A). Above 30 km, winter stratospheric temperatures are too warm to support PSCs, and this altitude roughly marks the top of the highly isolated region of the polar vortex.

The meridional gradients in concentration of various chemical tracers observed in midwinter and spring at the vortex boundary are

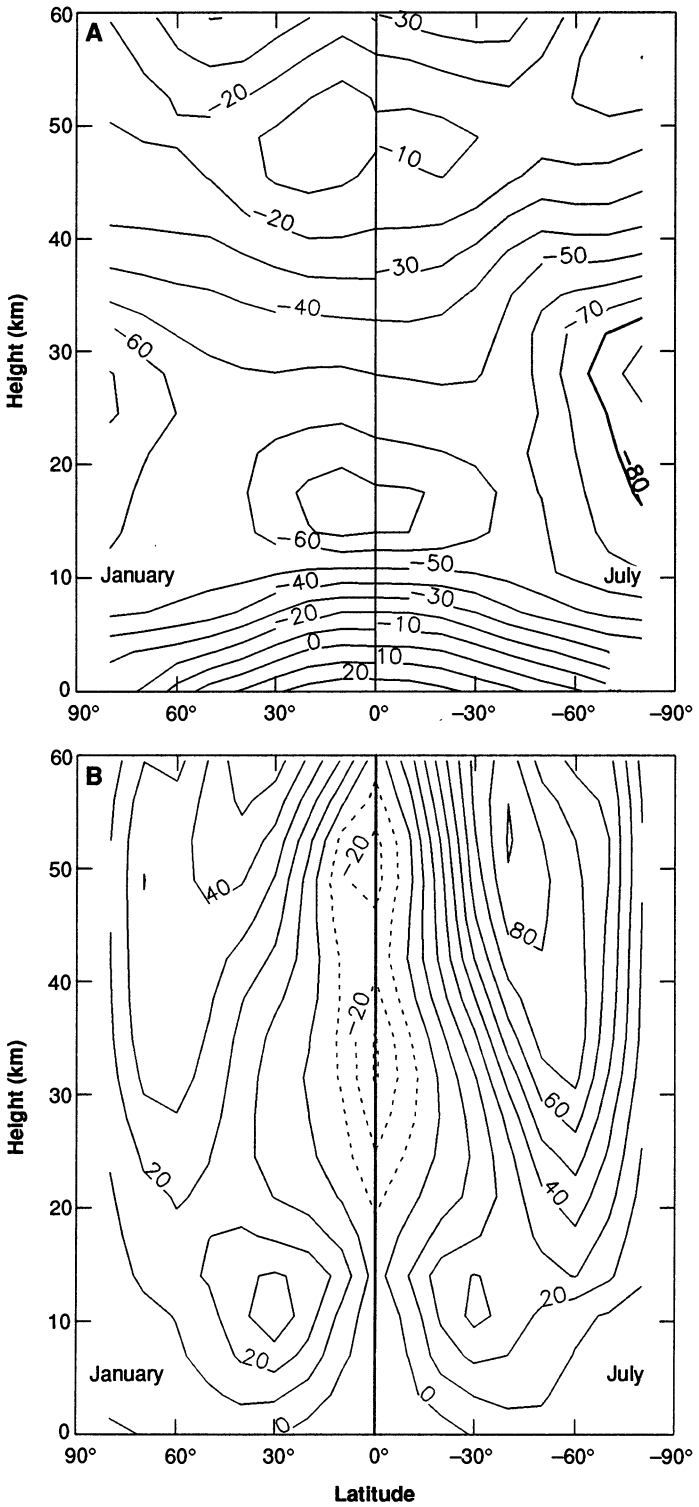

Fig. 2. Temperature (in centigrade) (**A**) and westerly wind speed (in meters per second) (**B**) observations averaged around latitude circles for the winter months of January in the Northern Hemisphere and July in the Southern Hemisphere. The data thus show the corresponding winter seasons in both hemispheres. Data are from (*10*). Temperatures below −80°C (enclosed with a heavy contour) are preferential sites for PSC formation.

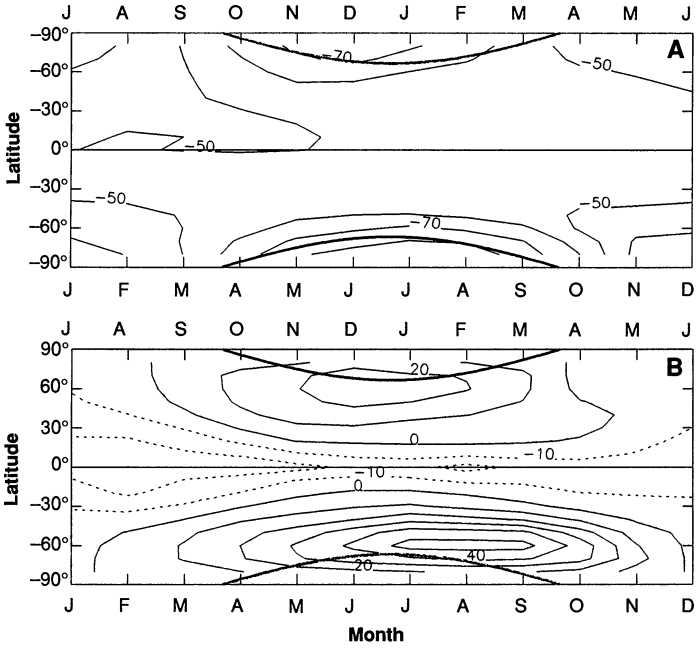

Fig. 3. Time evolution of the temperatures (**A**) and zonal winds (**B**) in the lower stratosphere (24 km, 30 mb). Northern Hemisphere data are shifted by 6 months to facilitate comparison. The heavy solid line marks the edge of polar night. Data are from (*10*).

much sharper than would be expected from simple symmetric overturning or the latitudinal variation of radiative-equilibrium temperatures. Both recent polar stratospheric aircraft missions show that these tracer gradients are very sharp: the entire transition from mid-latitude to polar air characteristics takes place over a distance of several hundred kilometers (*12*). The sharp gradient in long-lived tracers provides a consistent marker of the edge of the polar vortex for periods of a month or more (*13*) and is a further indicator of the ability of the polar vortex to inhibit mixing (*14*). As discussed below, the sharpening of the meridional constituent gradient across the vortex edge appears to be directly related to the planetary wave erosion of the vortex edge.

In the spring, solar heating of ozone returns to the polar regions, and the meridional temperature gradient begins to weaken (Fig. 3). The vortex wind system appears to transit abruptly to the summer circulation by way of an event called a final stratospheric warming. During the final warming, amplitudes of planetary wave displacement increase explosively, and the vortex shatters into smaller fragments that drift to mid-latitudes. These fragments still contain the chemically perturbed inner vortex air, including any ozone depletions that may have occurred, and can persist for weeks (*15*). The final warming usually develops in March in the Northern Hemisphere but may be as late as early December in the Southern Hemisphere. The reduced solar heating of ozone as a result of ozone depletion has been implicated in delaying the Austral final warming in 1987 (*16*). The stratospheric summer circulation is composed of weak easterly winds flowing symmetrically about the pole.

Physics of the Polar Vortex

Early models of the polar vortex were designed to investigate the sudden warming events and considered a single planetary wave propagating in a basic state vortex (*17*). With the advent of stratospheric global satellite observations in the last 10 years, a more synoptic picture of vortex development and decay has emerged. This synoptic viewpoint has been sharpened by the widespread use of potential vorticity (*PV*) as a flow diagnostic (*18*). Potential vorticity is the dot product of the absolute vorticity vector and the gradient of a conservative thermodynamic property. *PV* is conserved for adiabatic, frictionless flows. The thermodynamic variable most often chosen is potential temperature (*19*). If we use potential temperature as the vertical coordinate, then *PV* has a simple scalar definition: it is the sum of the planetary vorticity, f (due to Earth's rotation), and z, the local vertical component of the curl of the velocity field measured on a potential temperature surface, multiplied by a lapse rate factor, S

$$PV = (f + z)S \quad (2)$$

The lapse rate factor is a measure of the vertical distance between isentropic (potential temperature) surfaces (*20*), which are material surfaces for adiabatic flow. This factor accounts for the increase or decrease in vorticity that can occur when fluid tubes become vertically stretched or compressed. Because *PV* is conserved for most real atmospheric flows and because it can be derived from a field of temperature observations, it becomes a powerful diagnostic for transport of trace species (*21*).

As the vortex spins up in early winter, *PV* builds up rapidly in the polar region and the *PV* gradient between the subtropics and the pole increases. [*PV* is not conserved under the diabatic seasonal change in insolation, although some important *PV* conservation theorems still hold (*21*).] The positive *PV* gradient is required for the existence of planetary waves, which are essentially oscillations between the relative and planetary components of vorticity. Planetary waves propagate into the vortex along the *PV* gradient and are refracted toward low latitudes (*22*). Because the energy of vertically propagating planetary waves is nearly conserved along the direction of propagation, their amplitude increases as the density decreases with altitude. Eventually the wave amplitudes become large enough to overcome the mean *PV* gradient, and the waves then "break," laterally rotating the north-south *PV* gradient and causing irreversible mixing of *PV* and attendant chemical species (*23*). The poleward transport of heat during a wave-breaking event causes a stratospheric warming.

Because of the equatorward propagation of planetary waves, planetary wave breaking and associated constituent mixing occurs preferentially on the equatorward edge of the polar vortex, where a mid-latitude "surf zone" is created (*23*). The surf zone or rapid-mixing region effectively flattens the *PV* pole-to-equator gradient at mid-latitudes while steepening the gradient at the edge of the surf zone. The process is analogous to the strengthening of constituent gradients at the edge of turbulent regions (*24*).

Stratospheric major midwinter warmings usually begin with a displacement of the vortex from the pole toward mid-latitudes, or sometimes the vortex is split into lobes. Even during the warming the air in the vortex remains isolated as erosion of *PV* and trace species from the edge of the vortex sharpen the gradient. During the warming, the area covered by the high *PV* region rapidly decreases because of the erosion. After a midwinter stratospheric warming, the system usually recovers somewhat as the smaller vortex moves back to its polar position.

It is the increased number of the stratospheric warmings or erosion events in the Northern Hemisphere compared to those in the Southern Hemisphere that is responsible for the interhemispheric differences in the extent of the vortex (Figs. 1 and 2). The overall frequency of wave breaking events also determines the effective isolation of the vortex air. For this reason, the most isolated region of the vortex begins a few kilometers above the tropopause (as the influence of tropospheric weather systems dies out) and ends at about 30 km, above which planetary wave breaking is more frequent (*25*). The position of the upper vortex boundary will, of

course, change from year to year depending on the interannual variability of planetary wave activity. Midwinter stratospheric warming events are intermittent, occurring once or twice a season in the Northern Hemisphere but rarely in the Southern Hemisphere (*3*).

The erosion of the vortex and the sharpening of gradients along the edge of the polar vortex associated with the mid-latitude wave breaking have been dramatically illustrated with high-resolution computer models (*26*). These models, which usually use two-dimensional (latitude-longitude) representations of flow along an isentropic surface, show that little mid-latitude air penetrates to the vortex interior but that material along the vortex edge continues to be eroded into filaments that are rapidly mixed into mid-latitudes. These models appear to give a good representation of the overall vortex erosion process as observed in the stratosphere, and their results suggest that it is the more rapid erosion of the vortex by the planetary waves in the Northern Hemisphere that shifts this system away from the near–radiative equilibrium path characteristic of the Southern Hemisphere stratosphere (Fig. 3) (*27*).

Aircraft Observations

High resolution computer simulations of the polar vortex show fine-scale features and processes that cannot be resolved with observational analyses of stratospheric flow patterns based on balloon or satellite data. Almost at the same time that the first high-resolution model results were being published (*26*), the Airborne Antarctic Ozone Experiment (AAOE) was investigating the Antarctic ozone depletion using specially equipped ER-2 and DC-8 aircraft (*28*). A second expedition, the Airborne Arctic Stratospheric Expedition (AASE), investigated the Arctic polar vortex in January and February 1989 using the same aircraft (*29*).

During AAOE, the high altitude ER-2 was able to fly within the Antarctic ozone hole and obtain in situ measurements. The ER-2 made nearly continuous observations of N_2O (a long-lived trace gas), O_3, ClO, winds, temperature, and lapse rate. From the meteorological variables, *PV* can be estimated.

The data from the ER-2 show clear evidence of coincident, sharp gradients in N_2O and *PV*, both of which should be conserved on advective time scales in the polar stratosphere (Fig. 4). The sharp decline of N_2O and the increase of *PV* toward the pole are both indicative of the combined effects of the downward displacement of air inside the vortex and subsequent enhancement of the gradient by erosion of the outside edge of the vortex. This sharpened gradient structure is consistent with expectations derived from theory and high-resolution numerical models but is not captured in global meteorological analyses with coarser resolution.

In the polar vortex, the region where O_3 can be removed most rapidly is coincident with the region of high ClO. This region, sometimes called the chemically perturbed region (CPR), lies inside the vortex but does not coincide exactly with the edge of the vortex as defined by the steepening of the N_2O gradient (Fig. 4A). For both the Antarctic and Arctic data, ClO increases slightly just poleward of the relatively sharp decrease in N_2O (60°S in Fig. 4A; 68°N in Fig. 4B). A second larger increase in ClO, defining the CPR edge, occurs in the Antarctic data at 66°S, coincident with a second smaller decrease in N_2O. This large ClO change coincides with the region where temperatures are consistently below −75°C and PSC formation is more or less continuous. The DC-8 measurements indicate that $ClONO_2$ is anomalously high equatorward of the CPR, and NO_2 also increases rapidly there as well, although HCl is still low (*30*). Clearly, the active nitrogen species in the region between the dynamical edge of the vortex at 60°S and the CPR at 66°S are not suppressed. This region retains an abundance of active

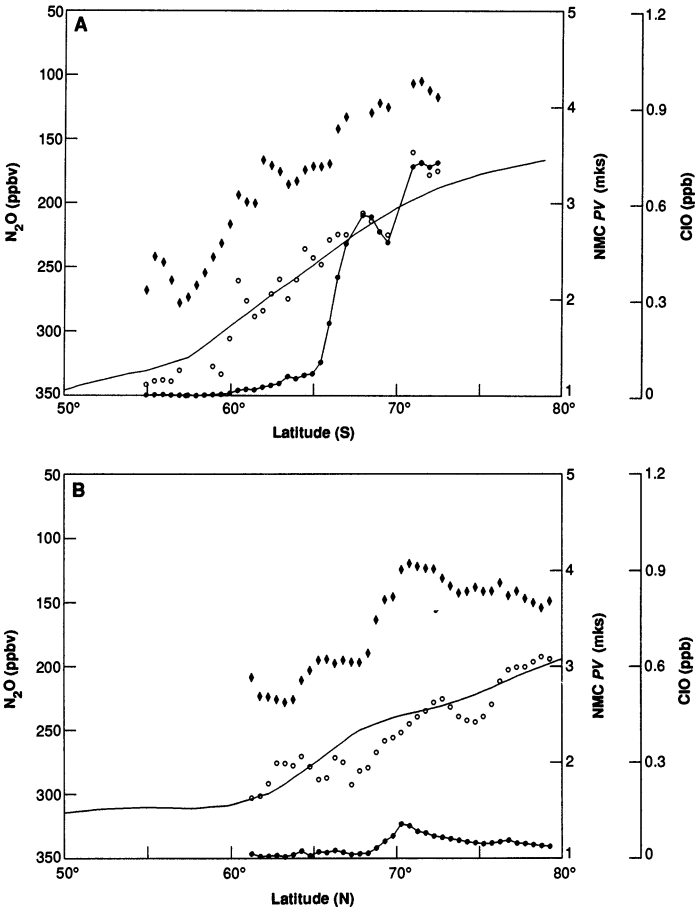

Fig. 4. The structure of the Antarctic (**A**) and Arctic vortex (**B**) as observed by high-altitude aircraft near 20 km. The diamonds are measured N_2O averaged into 0.5° latitude and 16 K potential temperature bins. The inside of the vortex is the region poleward of the sharp decrease in N_2O (low values are at the top of the graph). The connected data points show ClO. High abundances of ClO indicate the presence of chemically perturbed air in the vortex. The thin line is potential vorticity derived by the authors from National Meteorological Center gridded global analysis. The small circles show potential vorticity derived from the aircraft data. Potential vorticity is defined as a positive quantity in both hemispheres in these figures.

nitrogen radicals so that any ClO formed heterogeneously will recombine with ambient NO_2 and thus return chlorine to the reservoir $ClONO_2$. The region between the Austral vortex edge and the CPR appears to be chemically more characteristic of the Arctic vortex.

Chlorine monoxide formation in the Arctic vortex (Fig. 4B) appears to be associated with PSC events rather than with the continuous processing that occurs deep inside the Antarctic vortex. These PSC events are associated with the temporary cooling of air parcels to temperatures below the PSC condensation point through adiabatic expansion. For example, tropospheric cyclones can produce an upward bulge in the tropopause. This bulge acts like an orographic feature and results in adiabatic expansion, cooling, and stratospheric PSC formation as air passes over the bulge. During AASE, dramatic PSC events occurred near the edge of the vortex as a result of tropospheric cyclones (*31*). Such PSC events may be the most important Arctic and extra-CPR Antarctic ClO production mechanism because 50-mb average temperatures in these regions are usually above −78°C. The PSC events in the Antarctic vortex are often associated with the growth of cyclones near the Ross Sea (*32*).

Potential vorticity calculated from the global National Meteorological Center analysis only approximates the variations seen in N_2O (Fig. 4), but *PV* estimates from aircraft meteorological data show a

better correspondence with N_2O. Analysis of the AAOE and AASE data show that N_2O and *PV* provide consistent information about relative position in the vortex and can be used as surrogates (*33*). The aircraft observations of steep gradients at the edge of the polar vortex verify the predictions from high-resolution numerical models. Furthermore, the presence of sharp gradients implies that mixing across the vortex "wall" is limited because such sharp gradients can only occur at the edge or outside of vigorous mixed regions (*14*). This result means that the region of ozone depletion is not a lateral "flow-through reactor" for a large volume of stratospheric air. Nor can a significant amount of air enter through the top of the isolated region without disturbing the near–radiative equilibrium conditions in the vortex. It is possible that some lateral air exchange may occur near the tropopause through the action of tropospheric systems penetrating into the stratosphere, but this process has not been quantified (*34*). The effect of the ozone hole cannot be felt at mid-latitudes until the vortex breaks up (*14*).

Year-to-Year Variability in the Polar Vortex

The year-to-year variability of planetary wave activity in both hemispheres produces a corresponding response in the strength and temperature of the polar vortex. These year-to-year fluctuations in the vortex strength and temperature appear to dominate over the slow increase in available stratospheric Cl in determining the year-to-year variability of the severity of the ozone hole. Studies indicate that year-to-year variations in planetary wave activity generally follow the phase of the quasi-biennial oscillation (QBO) in the tropical winds at the lower stratosphere, with more activity during easterly phase years, and that the ozone hole tends to exhibit the same variability (*35*). For example, in the QBO westerly year of 1987, the ozone destruction in the Antarctic lower stratosphere was almost complete (*36*). In the QBO easterly year of 1988, the planetary wave activity was high, polar temperatures were warm, and the zonal mean vortex winds were weak (Fig. 5). In October 1988 the ozone depletion was much less than in 1987 (*37*).

The sensitivity of the ozone hole to dynamical activity is not unexpected because slight modulation of the vortex temperatures by planetary waves could greatly modulate the regional coverage of PSCs. Indeed, any planetary wave activity at all will tend to weaken the ozone depletion by raising the vortex temperatures (*38*).

Implications for the Future

One of the most important questions is: Are the polar ozone holes going to increase in size? The Antarctic ozone hole depletion is principally confined to the region inside the polar vortex where lower stratospheric temperatures remain below about −78°C for several months and PSCs are frequently observed. The areal extent of the −78°C region is determined by planetary wave activity that takes place during the fall and winter, before the springtime ozone depletion begins. Thus the maximum size of the Antarctic ozone hole would appear to be fixed first by the size of the core of cold temperatures in the vortex, which locates the CPR, and then by the dynamical boundary of the polar vortex as defined by the edge in the N_2O. Radiative transfer computations indicate that the 1987 Antarctic vortex approached radiative equilibrium (*39*), meaning that dynamical heat transport was very weak. Analysis of trace constituent data from aircraft also indicates that mixing was weak in 1987 (*14*). It is therefore doubtful that the areal extent of the pool of cold air in the vortex could increase beyond that observed in 1987 through purely dynamical mechanisms.

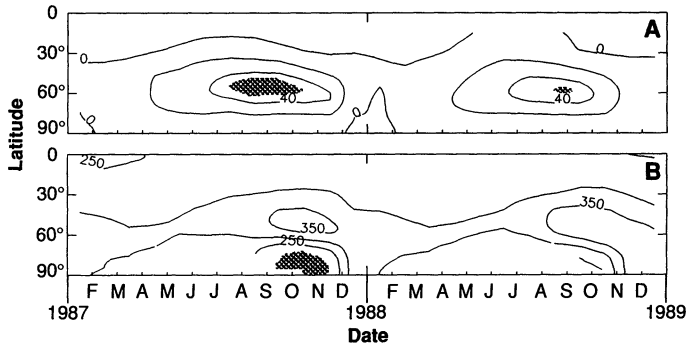

Fig. 5. Two years of 50-mb (20 km) stratospheric zonal wind data (**A**) and zonal mean total ozone data (**B**) in the Southern Hemisphere. Shading denotes the 200-DU boundary of the ozone hole and wind values of 50 m s^{-1}. Winter winds are strongest in the year when a severe spring ozone depletion develops. Ozone contours end in the polar night region where the satellite cannot take data.

However, there is another possibility for expansion of the ozone hole. In the Arctic, ozone depletion occurs in regions where PSC appearance is more episodic than continuous. It is also clear that the region between the Antarctic CPR and the vortex boundary has been exposed to heterogenous chemistry, as indicated by slightly elevated ClO levels and perturbed chlorine nitrate and HCl concentrations there (*30*). There may also be evidence of ozone depletion in that region (*40*). The present chemical perturbation of the Arctic and extra-CPR Antarctic depletions result from intermittent PSC appearance associated with troposphere cyclonic uplift or internal gravity waves.

As the concentration of reservoir chlorine compounds in the stratosphere continues to increase, this intermittent processing will generate a higher concentration of chlorine radicals and thereby lead to increased ozone destruction. Thus the Arctic vortex and the region outside the Antarctic CPR will likely show increased ozone loss in the next 10 years. If the Antarctic ozone depletion reaches the dynamical vortex boundary, then the ozone hole will effectively double in area because the chemically perturbed region currently occupies only about half the present area of the Antarctic vortex.

The Arctic vortex covers about half the area of the Antarctic vortex in the respective spring seasons when the ozone depletion occurs, and the coldest regions are between 20 and 50 mb. If ozone were totally removed from that region, the ozone column would experience only about 40% of the decrease observed in the 1987 Antarctic depletion (roughly 40 Dobson units). Thus the most severe Arctic ozone hole will never rival the current Antarctic depletions unless stratospheric climate or water vapor content changes (*41*).

Stratospheric climate is controlled principally by the radiative balance between heating through absorption of ultraviolet radiation by ozone and CO_2 cooling through emission of infrared radiation. In order to produce more substantial ozone depletions in springtime by the mechanisms involving PSCs, the polar vortex must become colder, larger, or more persistent. It can become colder through radiative processes, either through reduced solar absorption by ozone, or by more efficient emission of thermal energy by CO_2 or water vapor. Atmospheric CO_2 is increasing as a result of fossil fuel burning and other causes, and as it increases the stratosphere will cool (*42*). A similar effect will occur as global stratospheric ozone decreases. Methane, an important source of water in the stratosphere, is also increasing in the atmosphere, and increased water vapor would increase the probability of PSC formation (*43*). While these mechanisms for enhancing the polar ozone depletions are plausible qualitatively, their quantitative effect is probably rather small, at least during the next couple of decades. The greatest

impediment to a strengthened Arctic vortex, and hence to a significant amplification of the Arctic ozone hole, is the vigorous mixing provided by the planetary waves that propagate upward from sources in the troposphere. The generation of large-amplitude planetary waves is intermittent—one might even say chaotic—and such chaotic generation leads to substantial interannual variability in the strength and longevity of the Arctic polar vortex. A significant change in the amount of planetary-wave stirring provided from the troposphere to the stratosphere is unlikely, although the possible development of such a trend as the stratosphere cools because of the increasing levels of greenhouse gases cannot be ruled out.

REFERENCES AND NOTES

1. Steady zonally symmetric circulations over large meridional scales cannot maintain angular momentum balance without additional momentum sources or friction. Where such circulations occur, momentum balance is supplied by dissipating atmospheric waves or surface drag.
2. J. C. Charney and P. G. Drazin, *J. Geophys. Res.* **66**, 83 (1961).
3. For example, see M. R. Schoeberl, *Rev. Geophys.* **16**, 521 (1978).
4. Stratospheric lenticular lee-wave clouds are called nacreous clouds, which were first described by Norwegian meteorologists. These clouds tend to form in the 15- to 30-km region of stratosphere and are apparently associated with substantial orographic uplift and rapid cooling found in lee waves. The size of the ice crystals in nacreous clouds is uniformly 1 to 2 μm in diameter leading to an unusual pearly or nacreous appearance in sunlight. These clouds and other types of PSCs can be observed by satellite with solar occultation techniques [M. P. McCormick and C. R. Trepte, *J. Geophys. Res.* **92**, 4297 (1987)].
5. P. Hanson and K. Mauersberger, *Geophys. Res. Lett.* **15**, 855 (1988).
6. For a review see S. Solomon, *Rev. Geophys.* **26**, 131 (1988). The earliest seminal papers on PSCs and the perturbed chemistry of the ozone hole include S. Solomon, R. R. Garcia, F. S. Rowland, D. J. Wubbles, *Nature* **321**, 755 (1986); M. B. McElroy, R. J. Salawitch, S. C. Wofsy, J. A. Logan, *ibid.*, p. 759; O. B. Toon, B. P. Hamill, R. P. Turco, J. Pinto, *Geophys. Res. Lett.* **13**, 1284 (1986). More recently, D. W. Fahey *et al.* [*J. Geophys. Res.* **94**, 11299 (1989)] discuss PSC measurements in the Antarctic.
7. L. T. Molina and M. J. Molina [*J. Phys. Chem.* **91**, 433 (1987)] first pointed out the importance of the reaction forming the $(ClO)_2$ dimer in polar ozone destruction; for more recent measurements of the dimer formation rate and a discussion of the photochemistry see S. P. Sander, R. R. Friedl, and Y. L. Yung [*Science* **245**, 1095 (1989)] and J. M. Rodriguez, M. K. W. Ko, and N. D. Sze [*Geophys. Res. Lett.* **17**, 255 (1990)].
8. J. G. Anderson *et al.*, *J. Geophys. Res.* **94**, 11480 (1989).
9. During the AASE mission the ER-2 detected ClO mixing rations approaching those found in the Antarctic ozone hole [W. L. Brune, D. W. Toohey, S. A. Lloyd, J. G. Anderson, *Geophys. Res. Lett.* **17**, 505 (1990)]. Arctic ozone loss of about 0.5% per day has been reported (M. R. Schoeberl *et al.*, *ibid.*, p. 469). This should be compared to the Antarctic ozone losses of 1 to 2% per day (*34*).
10. E. L. Fleming, S. Chandra, M. R. Schoeberl, J. J. Barnett, *NASA Tech. Memo. 100697* (1988).
11. S. B. Fels, *Adv. Geophys.* **28**, 277 (1985).
12. M. Loewenstein, J. R. Podolske, K. R. Chan, S. E. Strahan, *J. Geophys. Res.* **94**, 11589 (1989); L. R. Lait *et al.*, *Geophys. Res. Lett.* **17**, 521 (1990).
13. M. H. Proffitt *et al.*, *J. Geophys. Res.* **94**, 11437 (1989).
14. D. L. Hartmann *et al.*, *ibid.*, p. 16779.
15. Fragments of ozone-depleted air from the 1987 ozone hole were detected over Australia and New Zealand in December after the late November vortex breakup [R. J. Atkinson, W. A. Mathews, P. A. Newman, R. A. Plumb, *Nature* **340**, 290 (1989)]. Simulations of the vortex breakup and the chemical evolution performed by M. Prather and A. H. Jaffe [*J. Geophys. Res.* **95**, 3473 (1990)] appear to be consistent with these observations.
16. J. T. Kiehl, B. A. Boville, B. P. Briegleb, *Nature* **332**, 522 (1988).
17. T. Matsuno, *J. Atmos. Sci.* **28**, 1479 (1971); J. R. Holton, *ibid.* **33**, 1639 (1976).
18. B. L. Hoskins, M. E. McIntyre, A. W. Robertson, *Q. J. R. Meteorol. Soc.* **111**, 877 (1985).
19. Derivation of Ertel's theorem and the definition of Ertel's potential vorticity (or just potential vorticity) is given in many textbooks [J. Pedlosky, *Geophysical Fluid Dynamics* (Springer-Verlag, New York, 1986)]. Potential temperature is the temperature of an air parcel brought adiabatically to the surface. For example, in the polar vortex, the 50-mb pressure surface corresponds approximately to the 180°C potential temperature surface even though the actual temperature on that surface is about −80°C.
20. Potential vorticity is usually defined as $Q = -g(f + z) \cdot d(\theta)/dp$ where g is the acceleration due to gravity and θ is the potential temperature (*19*).
21. P. H. Haynes and M. E. McIntyre, *J. Atmos. Sci.* **44**, 828 (1987).
22. D. J. Karoly and B. J. Hoskins, *J. Meteorol. Soc. Jpn.* **60**, 109 (1982).
23. M. E. McIntyre and T. N. Palmer, *J. Atmos. Terr. Phys.* **46**, 825 (1984).
24. Most people do not think of the nonlinear mixing by 1000-km scale waves as turbulence; nonetheless, all zonal mean stratospheric chemical models parameterize planetary wave transport with the use of simple diffusion-coefficient and mixing-length analogues. These coefficients can be derived from observational data [P. A. Newman, M. R. Schoeberl, R. A. Plumb, J. E. Rosenfield, *J. Geophys. Res.* **93**, 5221 (1988)].
25. T. J. Dunkerton and D. P. Deleisi, *J. Geophys. Res.* **91**, 1199 (1986); M. R. Schoeberl and A. K. Smith, *J. Atmos. Sci.* **43**, 1074 (1986).
26. M. N. Jukes and M. E. McIntyre, *Nature* **328**, 590 (1987); M. L. Salby and R. R. Garcia, *Phys. Today* **43**, 38 (1990); similar results have also been obtained with a three-dimensional model [J. D. Mahlman and L. J. Umcheid, in *Transport Processes in the Middle Atmosphere*, G. Visconti and R. Garcia, Eds. (Reidel, Boston, 1986), pp. 251–266.]
27. The effectiveness of the planetary wave–vortex erosion processes compared to simple radiative deceleration of the vortex by the increasing spring insolation has been clearly demonstrated [N. Buchart and E. E. Remsburg, *J. Atmos. Sci.* **28**, 1087 (1986)].
28. A. F. Tuck, R. T. Watson, E. P. Condon, J. J. Margitan, O. B. Toon, *J. Geophys. Res.* **94**, 1181 (1989).
29. R. Turco, A. Plumb, E. Condon, *Geophys. Res. Lett.* **17**, 313 (1990).
30. G. C. Toon *et al.*, *J. Geophys. Res.* **94**, 16571 (1989).
31. P. A. Newman, personal communication.
32. The stratospheric clouds formed by these events produce retrieval anomalies in the Total Ozone Mapping Spectrometer satellite data that look like small ozone holes or "mini-holes" [P. A. Newman, L. R. Lait, M. R. Schoeberl, *J. Geophys. Res.* **93**, 923 (1988); D. S. McKenna *et al.*, *ibid.* **94**, 11641 (1989)].
33. D. L. Hartmann *et al.*, *ibid.*, p. 11669; M. R. Schoeberl *et al.*, *ibid.*, p. 16815 and unpublished analysis of AASE observations by the authors.
34. There is still some debate about the extent to which air moves through the Antarctic vortex [M. L. Proffitt *et al.*, *J. Geophys. Res.* **94**, 16797 (1989); A. F. Tuck, *ibid.*, p. 11687], but the overall exchange of air is certainly smaller than the overall mass of ozone-depleted air within the vortex (*14*). The ozone hole occupies about 7.5% of the area of the Southern Hemisphere and extends from roughly 100 to 30 mb. This is about 2.6% of the mass of the stratosphere.
35. The correlation of Antarctic ozone depletion with the QBO was first pointed out by R. R. Garcia and S. Solomon [*Geophys. Res. Lett.* **14**, 848 (1987)]. A more recent quantitative study can be found in L. Lait, M. R. Schoeberl, and P. A. Newman [*J. Geophys. Res.* **94**, 11559 (1989)]. While the westerly phase QBO–large ozone depletion correlation generally holds, there are notable exceptions, such as spring 1989 when the QBO winds were in the easterly phase but late winter planetary wave activity was low. The resultant strong 1989 vortex provided ideal conditions for the development of a large ozone depletion [T. Deshler, D. J. Hofmann, J. V. Hereford, C. B. Sutter, *Geophys. Res. Lett.* **17**, 151 (1990); R. S. Stolarski, M. R. Schoeberl, P. A. Newman, R. D. McPeters, A. J. Krueger, *ibid.*, in press].
36. D. J. Hofmann, J. W. Harder, J. M. Rosen, J. V. Hereford, J. R. Carpenter, *J. Geophys. Res.* **94**, 16527 (1989).
37. M. R. Schoeberl, R. S. Stolarski, A. J. Krueger, *Geophys. Res. Lett.* **16**, 377 (1989).
38. L. R. Poole, S. Solomon, M. P. McCormick, M. C. Pitts, *ibid.*, p. 1157.
39. J. R. Rosenfield, personal communication.
40. M. H. Proffitt, D. W. Fahey, K. K. Kelly, and A. F. Tuck [*Nature* **342**, 233 (1989)] claimed that there is evidence for ozone loss outside the CPR; however, a number of authors have confused the edge of the CPR with the dynamical edge of the polar vortex as defined by the steep gradient in long-lived tracers (Fig. 3) [M. R. Schoeberl, *Eos* **70**, 1044 (1989)] so the results of Profitt *et al.* should not be interpreted as evidence for ozone loss outside the polar vortex.
41. This statement refers to ozone depletions produced by the heterogeneous PSC chemistry taking place in polar regions. As anthropogenic Cl continues to increase in the stratosphere, gas phase reactions will generate depletions in ozone outside the polar region. For the most recent assessments of global ozone depletion, see *Scientific Assessment of Stratospheric Ozone: 1989, World Meteorol. Org. Rep. 20* (1990).
42. Increases in CO_2 concentration are well documented [H. Oeschger and U. Siegenthaler, in *The Changing Atmosphere*, F. S. Rowland and I. S. A. Isaksen, Eds. (Wiley, New York, 1988), pp. 5–24]; doubling CO_2 levels should produce a 10°C decrease in stratopause temperatures [S. B. Fels, J. D. Mahlman, M. D. Schwarzkopf, R. W. Sinclair, *J. Atmos. Sci.* **37**, 2265 (1980)].
43. D. R. Blake and F. S. Rowland, *Science* **239**, 1129 (1988).

44. We thank J. D. Mahlman for helpful comments on this manuscript. We also thank all the instrument and theory teams associated with the AAOE and AASE aircraft missions for their hard work and dedication, and particularly the project scientist A. Tuck and project manager E. Condon. We thank L. R. Lait for production of Fig. 1, and M. Lowenstein and J. Anderson for the AASE and AAOE data in Fig. 4.